Top Catal (2017) 60:1735–1743
DOI 10.1007/s11244-017-0850-9

ORIGINAL PAPER

IR-Spectroscopic Study on the Interface of Cu-Based Methanol Synthesis Catalysts: Evidence for the Formation of a ZnO Overlayer

Julia Schumann[1,3,4] · Jutta Kröhnert[1] · Elias Frei[1] · Robert Schlögl[1,2] · Annette Trunschke[1]

Published online: 28 August 2017

Abstract Carbon monoxide was applied as probe molecule to compare the surface of a ZnO-containing (Cu/ZnO:Al) and a ZnO-free (Cu/MgO) methanol synthesis catalyst (copper content 70 atomic %) after reduction in hydrogen at 523 K by DRIFT spectroscopy. Nano-structured, mainly metallic copper was detected on the surface of the Cu/MgO catalyst. In contrast, the high energy of the main peak in the spectrum of CO adsorbed on reduced Cu/ZnO:Al (2125 cm^{-1}) proves that metallic copper is largely absent on the surface of this catalyst. The band is assigned to $Zn^{\delta+}$–CO. The presence of not completely reduced $Cu^{\delta+}$–CO species cannot be excluded. The results are interpreted in terms of a partial coverage of the copper nano-particles in the Cu/ZnO:Al catalyst by a thin layer of metastable, defective zinc oxide. Minor contributions in the spectrum at 2090 and 2112 cm^{-1} due to nano-structured Cu^0–CO and CO adsorbed on highly defective Cu^0, respectively, indicate that the coverage of metallic copper is not complete.

Keywords Cu · Methanol synthesis catalyst · CO adsorption · DRIFTS

1 Introduction

Climate change and the limited availability of fossil fuels drive the development of renewable energy sources. The fluctuations of renewable energy require efficient energy storage for a viable renewable future energy scenario. One promising possibility is the conversion of electrical energy into chemical energy in molecules such as methanol using CO_2 as feedstock. Despite the large-scale application of methanol synthesis over $Cu/ZnO/Al_2O_3$ catalysts for several decades, understanding of the unique Cu–ZnO synergy that renders this catalyst active is still incomplete. However, this understanding is crucial in order to optimize the catalyst to the special conditions needed for methanol synthesis from a CO_2 based feed and to application under dynamic operation conditions.

Infrared spectroscopy is a powerful tool to investigate oxides or supported metal catalysts [1–4]. Indirect information concerning nature and number of adsorption sites at the surface of the catalyst is retrieved by adsorption of appropriate probe molecules. Carbon monoxide has been used frequently as a probe molecule based on non-reactive adsorption at cationic sites, [4] the formation of carbonyls with metals, [5, 6] and the weak interaction with hydroxyl groups [2, 7]. Alterations of the probed surface by possible redox reactions of CO with surface sites or the formation

In memoriam Prof. Dr. Helmut Knözinger.

Electronic Supplementary Material The online version of this article (doi:10.1007/s11244-017-0850-9) contains supplementary material, which is available to authorized users.

✉ Elias Frei
efrei@fhi-berlin.mpg.de

✉ Annette Trunschke
trunschke@fhi-berlin.mpg.de

[1] Department of Inorganic Chemistry, Fritz-Haber-Institut der Max-Planck-Gesellschaft, Faradayweg 4-6, 14195 Berlin, Germany

[2] Max Planck Institute for Chemical Energy Conversion, Stiftstr. 34-36, 45470 Mülheim, Germany

[3] Present Address: Department of Chemical Engineering, Stanford University, 443 Via Ortega, Stanford, CA 94305, USA

[4] SLAC National Accelerator Laboratory, SUNCAT Center for Interface Science and Catalysis, 2575 Sand Hill Road, Menlo Park, CA 94025, USA

of volatile carbonyls [8] can be prevented by adsorption at liquid nitrogen temperature.

Due to the high copper content (50–70 wt%) in industrial relevant Cu/ZnO/Al_2O_3 (Al_2O_3 as phase, higher Al-content of 10–15 wt%) methanol synthesis catalysts, infrared studies of probe molecule adsorption on realistic systems and operando investigations are, however, limited [9–12]. Frequently, FTIR studies have been performed on model catalysts with lower copper contents or after dilution [13–19].

Recently, a Cu/ZnO:Al (Al as dopant in the ZnO; ZnO:Al, lower Al-content of <3 wt%) catalyst has been compared with a Cu/MgO catalyst in methanol synthesis [20–22]. The Cu nano-structure in Cu/ZnO:Al and Cu/MgO is almost identical due to the common malachite-based precursor structure [20]. Despite similar Cu-content and specific surface area, the Cu/MgO catalyst showed a seven times higher activtiy in a CO/H_2 feed, [22] and almost no activity in a CO/CO_2/H_2-feed, confirming the needed Cu–ZnO synergy in particular for the CO_2 activation [23–28] that may be attributed to different reasons including a wetting of Cu by (layered-) ZnO under reaction conditions. The coverage of the Cu-surface by a ZnO overlayer, as possible reason for the poor activity in a CO/H_2 feed, has been recently visualized by high-resolution transmission electron microscopy (HR-TEM) studies of a reduced Cu/ZnO:Al catalyst [29]. Strong metal-support interaction (SMSI) is apparently implemented by the formation of a thin layer of metastable "graphitic -/boron nitride-like" ZnO on the surface of the copper particles after reductive activation of the catalyst.

Local insight into the nano-structure by electron microscopy is complemented in the present contribution by a diffuse reflectance infrared Fourier transform (DRIFT) spectroscopy study. Infrared spectroscopy of adsorbed carbon monoxide provides integral information regarding nature and abundance of adsorption sites. The surface of Cu/ZnO:Al and Cu/MgO catalysts are compared with a special focus on the metal/metal oxide interface and the accessibility of the Cu moieties.

2 Experimental

2.1 Catalyst Synthesis

Calcined CuO/ZnO:Al and CuO/MgO precursors that contain a similar amount of Cu were prepared by constant pH co-precipitation [20, 21]. The zincian malachite precursor with a Cu:Zn ratio of 70:30 and 3 mol% (metal base) Al was synthesized by co-precipitation from a Cu, Zn, Al nitrate solution (1 M metal-based) and a 1.6 M Na_2CO_3 solution as a basic precipitating agent in an automated laboratory reactor setup (Labmax, Mettler Toledo). While stirring at 300 rpm, the metal nitrate solution (600 g) was dosed at a temperature of 338 K. The pH was controlled by a feedback loop through simultaneous addition of the Na_2CO_3 solution at pH 6.5. After 30 min the dosing was complete. Ageing was pursued for 80 min, then the slurry was filtrated and the precipitate was washed until the conductivity of the filtrate was below 0.5 mS cm^{-1}. Spray-drying yielded the greenish-blue-colored precursor powder. For the preparation of the zinc-free Cu/MgO catalyst, a Cu, Mg nitrate solution with a Cu:Mg ratio of 70:30 was used. The co-precipitation was performed at pH 9. Subsequent synthesis steps were identical to the preparation of the Cu/ZnO:Al precursor.

The precursors were calcined in a rotary furnace in a flow of 125 mL min^{-1} of 20% O_2 in Ar at 603 K for 3 h and a heating rate of 2 K min^{-1}. Reduction of the calcined precursors was performed in-situ in the cell for DRIFTS measurements.

2.2 DRIFTS Measurement

Diffuse reflectance infrared Fourier transform (DRIFT) spectra were collected on a Cary 600 Series FTIR Spectrometer from Agilent Technologies equipped with a liquid nitrogen-cooled MCT detector at a spectral resolution of 2 cm^{-1} and accumulation of 512 scans. An in-situ cell (Harrick Praying Mantis™ diffuse reflectance attachment DRP-DF8 in combination with a low temperature CHC-CHA-3 reaction chamber) was used. Prior to the measurements the optical path was aligned. The contribution of specular reflected light directed to the detector was minimized by using a mirror in sample position.

Spectra were taken at 77 or 300 K, respectively, after appropriate pretreatment in the reaction chamber. The calcined precursors were dehydrated in the DRIFTS cell by treatment in 4% O_2 in Ar at 423 K. 5% H_2 in Ar gas flow was used to reduce the calcined precursors with a heating rate of 6 K min^{-1} up to 523 K. The temperature was kept at 523 K for 30 min, then hydrogen was switched off and the sample was cooled down to 298 K in Ar. At room temperature, the DRIFTS cell was evacuated until a pressure of 10^{-5} mbar. The spectra of the two catalysts after reduction measured in diffuse reflection using KBr as background are presented in the Supporting Information (Fig. S1). Despite the low reflectance (<0.1%) the quality of the spectra is high. Furthermore, the reflectance of the two reduced catalysts in the frequency range of C–O stretching vibrations ($2150-1950\ cm^{-1}$) is comparable.

The single-beam spectrum of the corresponding pretreated catalyst was used as background to generate the spectrum of adsorbed CO. The spectra of adsorbed CO are presented in Kubelka–Munk units $F(R_\infty)=(1-R_\infty)^2/2R_\infty$ [30–32]. CO isotherms were recorded by dosing CO at increasing equilibrium pressures ranging from 0.1 to

80 mbar. For each experiment a freshly pretreated sample was used.

3 Results

The general characteristics of the investigated samples within this DRIFTS study are summarized in Table 1. The nano-structure of copper oxide in the two calcined precursors is very similar leading to comparable Cu domain sizes in the reduced catalysts as revealed by XRD, regardless whether ZnO:Al or MgO was used as spacer. The XRD data are measured under in-situ conditions and the patterns are shown in the Supporting Information (Fig. S2). The Cu domain size is given as volume weighted (L_{VOL}-IB) and Scherrer-equation based FWHM values. The Cu surface area is determined with H_2-TPD measurement. The N_2O-surface area is in correlation to the redox active sites on the surface. That means if we have e.g. oxygen vacancies in the metal oxide component or the metal oxide is reducible, the N_2O and the H_2-TPD values are different. This is the case for Cu/ZnO:Al, but not for Cu/MgO. The reactivity data show very clearly that for a fast CO_2 hydrogenation ZnO has to be present and with a ZnO-free Cu/MgO only CO can be converted.

Table 1 Chemical composition, surface areas and particle size of Cu particles in Cu/ZnO:Al and Cu/MgO

	Cu/ZnO:Al	Cu/MgO
ID of calcined catalyst[a]	19,081	19,802
XRF metal-based (atom%)	68/29/3	70/30
BET precursor/calcined catalyst (m^2g^{-1})	128/123	114/116
Cu domain size reduced catalyst (nm)[b]	5.5/7.7	9.3/13.0
Cu particle size TEM (nm)	8.1 [21]	n.d.
Cu surface area N_2O (m^2g^{-1})	36 [33]	24 [33]
Cu surface area H_2 (m^2g^{-1})[c]	16 [33]	24 [33]
Catalytic activity [μmol_{MeOH} (g_{cat} min)$^{-1}$][d]	55	350
Catalytic activity [μmol_{MeOH} (g_{cat} min)$^{-1}$][e]	300	20

[a]required to clearly distinguish different batches of catalyst synthesis

[b]determined by in-situ XRD measurements as L_{Vol}-IB/L_{Vol}-FWHM

[c]surface area was determined assuming Cu:H_2 = 3:1 stoichiometry, according to [33]

[d]p = 30 bar, T = 503 K, feed 14% CO/59% H_2/rest He

[e]p = 30 bar, T = 503 K, feed 8% CO_2/6% CO/59% H_2/rest He

3.1 CO Adsorption at 300 K

3.1.1 CO Adsorption on the Calcined Precursors

Spectra of CO adsorbed on the calcined precursors CuO/ZnO:Al and CuO/MgO (calcination at 603 K in synthetic air), respectively, are shown in Fig. 1. Bands due to adsorbed CO appear at the same positions for the two calcined precursors: a main signal at ca. 2100 cm^{-1} with a small shoulder at 2135 cm^{-1}. The main peak shifts slightly from 2092/2093 cm^{-1} at very low CO coverage to higher wavenumbers with increasing CO coverage for both the ZnO-free and ZnO-containing calcined precursors.

The integrated CO bands were plotted against the respective equilibrium pressure to obtain CO adsorption isotherms. Adsorption isotherms normalized to full coverage ($\theta = 1$) are presented in the Supporting Information (Fig. S3, left). Both CuO/MgO and CuO/ZnO:Al display the same shape of the CO adsorption isotherm. The overall adsorption capacity is comparable, although slightly higher for CuO/MgO as it

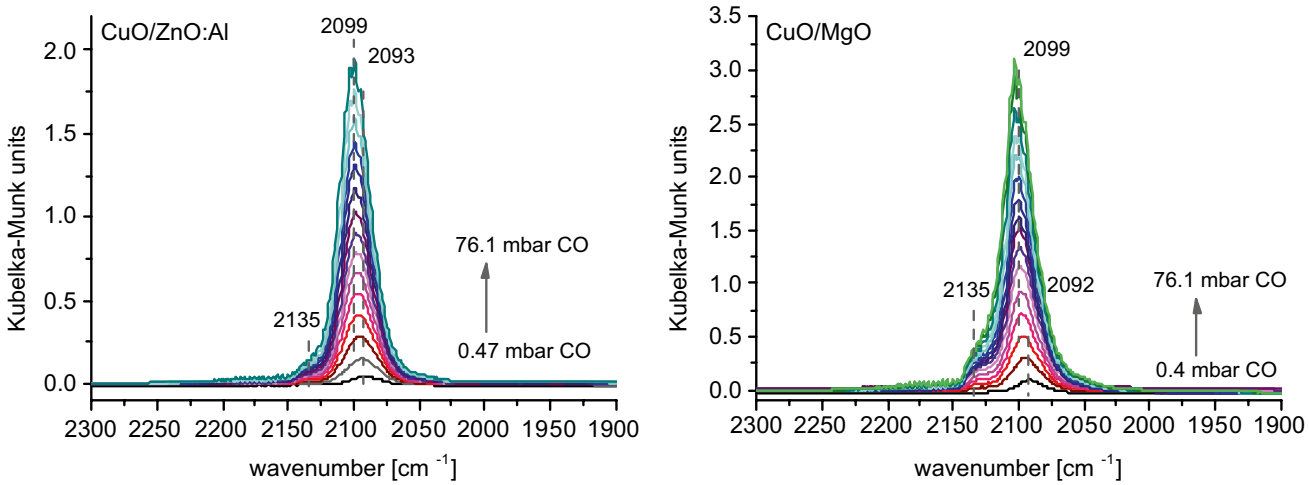

Fig. 1 Infrared spectra of CO adsorbed on the calcined precursors CuO/ZnO:Al (*left*), and CuO/MgO (*right*) after evacuation at 423 K (T_{ads} = 300 K, increasing equilibrium pressures from 0.5 to 76 mbar CO)

becomes apparent from the direct comparison at $\theta = 0.5$ in Fig. 5, left.

3.1.2 CO Adsorption at 300 K on the Reduced Catalysts

After reduction of the CuO containing calcined precursors in hydrogen containing feed at 523 K to bulk Cu metal, the CO band positions and adsorption capacity of the ZnO-containing and ZnO-free sample differ significantly (Fig. 2). The corresponding adsorption isotherms are shown in Fig. S3, right. The raw data (adsorption isotherms not normalized) are additionally presented in Fig. S4.

CO bands of the ZnO-free sample Cu/MgO (Fig. 2, right; Fig. 5, middle) appear mainly below 2100 cm^{-1}. The main band is located at 2089 cm^{-1}. With increasing coverage a shoulder at 2077 cm^{-1} develops that is shifted to 2060 cm^{-1} at $\theta = 1$. No blue shift is observed with increasing coverage.

The overall intensity of the absorption bands of the ZnO containing Cu/ZnO:Al catalyst is much weaker compared to Cu/MgO (Fig. 2, left). More important, the main signal appears here at 2125 cm^{-1}. At low coverage a signal at 2112 cm^{-1} can be distinguished with only very weak features at lower wavenumbers around 2090 cm^{-1}. With increasing pressure, the gas phase CO vibration and a weak band at 1996 cm^{-1} become visible.

Direct comparison of the two catalysts at 50% coverage is shown in Fig. 5 (middle). This figure clearly depicts the diminished adsorption capacity of the Cu/ZnO:Al catalyst and the differences in the band positions.

3.1.3 CO Desorption Experiments at 300 K on the Reduced Catalysts

Bands due to CO adsorption disappear rapidly upon evacuation at 300 K for both catalysts (Fig. 3). CO is slightly stronger adsorbed on Cu/MgO. After 3.5 min no signal due to CO adsorption is seen for Cu/ZnO:Al, whereas for Cu/MgO a small signal can still be observed after 3.5 min in vacuum. The additional band at 1996 cm^{-1} only observed on Cu/ZnO:Al cannot be removed by evacuation at room temperature.

3.2 CO Adsorption at 77 K on the Reduced Catalysts

In addition to the measurements at 300 K, CO adsorption spectra of the reduced catalysts were also recorded at liquid N_2 temperature at 77 K (Fig. 4). The corresponding adsorption isotherms are presented in the Supporting Information (Fig. S5).

A band at 2091 cm^{-1} appears upon adsorption of CO on Cu/MgO (Fig. 4, right), similar like in the adsorption experiment at 300 K (Fig. 2, right). A shoulder is observed at lower wavenumbers at around 2060 cm^{-1}. Additionally, a weak signal arises at 2180 cm^{-1}. This signal was not observed at room temperature. With increasing CO coverage, the peak maxima do not shift, but a weak shoulder of the main signal appears at higher wavenumbers around 2114 cm^{-1}, much stronger pronounced compared to the spectra recorded at room temperature.

The CO adsorption spectra of the reduced ZnO-containing catalyst differ strongly from the measurement at room temperature and show an increase in the absolute signal intensity (Fig. 4, left). At low coverage a main signal arises at 2096 cm^{-1}. A weak signal is observed at

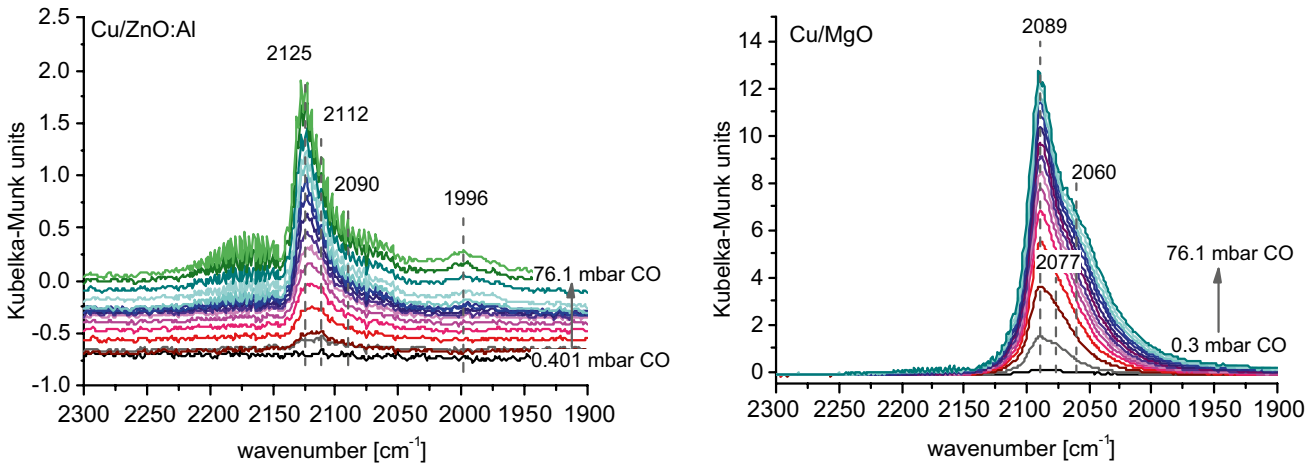

Fig. 2 Infrared spectra of CO adsorbed on the reduced catalysts Cu/ZnO:Al (*left*) and Cu/MgO (*right*) after reduction of the catalysts at 523 K in the infrared chamber ($T_{ads} = 300$ K, increasing equilibrium pressures from 0.3 to 76 mbar CO)

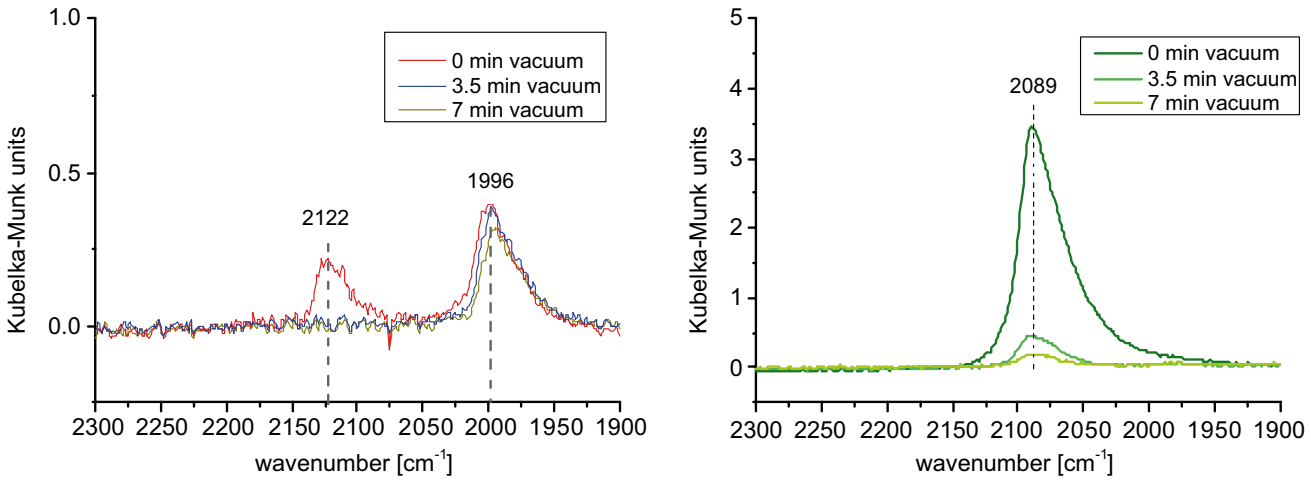

Fig. 3 Desorption of CO at 300 K on the reduced catalysts. *Left* Cu/ZnO:Al catalyst. *Right* Cu/MgO catalyst

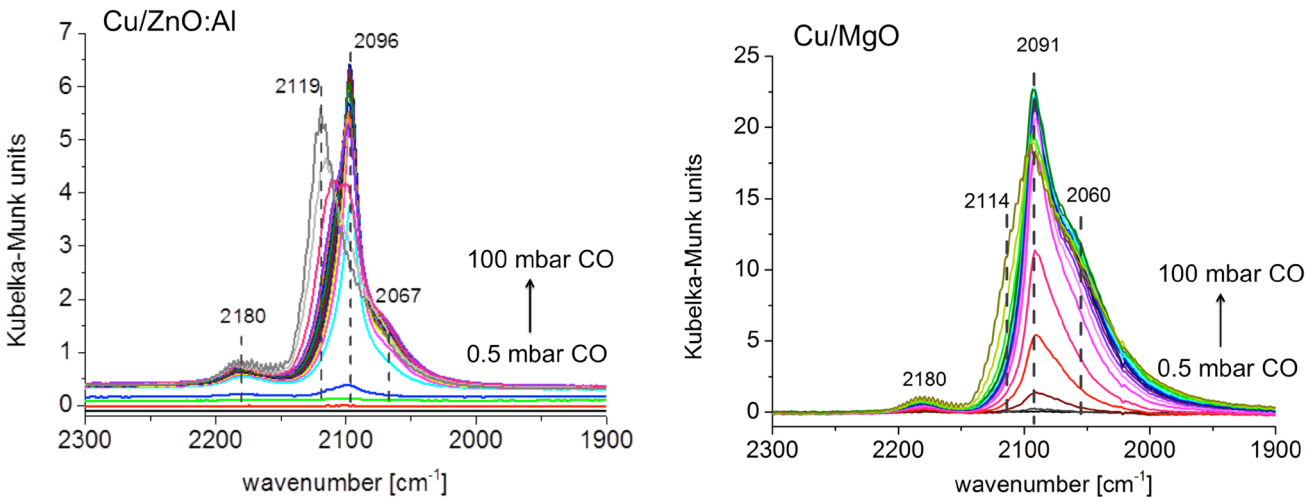

Fig. 4 Infrared spectra of CO adsorbed on Cu/MgO (*right*) and Cu/ZnO:Al (*left*) after reduction of the catalysts at 523 K in the DRIFTS cell (T_{ads} = 77 K, increasing equilibrium pressure from 0.1 to 58 mbar CO)

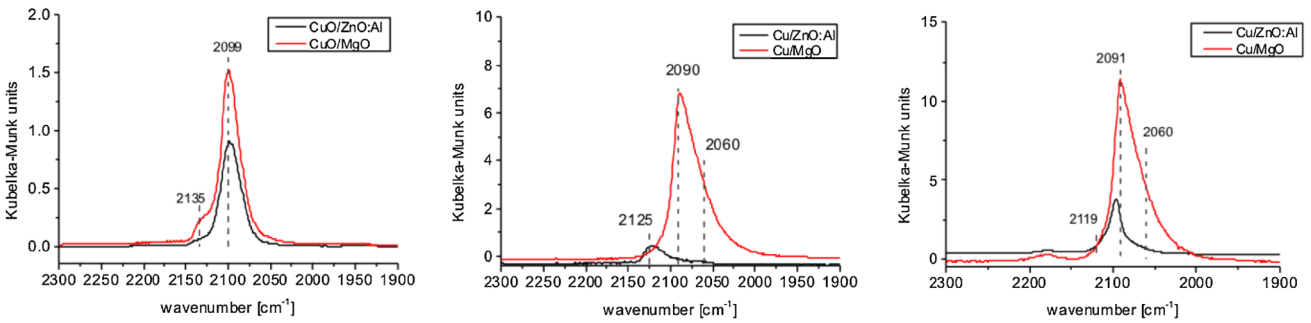

Fig. 5 DRIFT spectra of CO adsorbed at 300 K on the calcined precursors (*left*) and reduced catalysts (*middle*) and at 77 K on the reduced catalysts (*right*); the spectra have been recorded at a CO coverage of 0.5 ML

2180 cm^{-1}. Above a CO pressure of 5 mbar, the main signal at 2096 cm^{-1} decreases and a new signal at 2119 cm^{-1} arises and increases with increasing CO pressure.

3.3 CO Adsorption on Reference Oxides

CO was adsorbed on CuO and ZnO for reference (Fig. S6). CO adsorption at 300 K on CuO (Fig. S6, left) gives rise to CO stretching vibration at 2135 cm^{-1}. CO adsorption on ZnO is very weak. In order to obtain a measurable signal the adsorption was performed at liquid N_2 temperature (Fig. S6, right). A very weak signal at 2180 cm^{-1} was obtained.

4 Discussion

Assignment of CO band positions to Cu oxidation states and coordination numbers is by no means unambiguous and is further complicated by surface coverage dependencies of the band positions and the readiness of the Cu surface to react with CO [3]. The comparison of differently treated catalysts as well as the analysis of reference materials gave a better insight into the surface of ZnO-containing vs. ZnO-free Cu catalysts.

The stretching frequency regions of Cu^{n+}-CO surface carbonyl species with copper in different oxidation states overlap [3]. Generally, bands in the range $2220-2150\ cm^{-1}$ have been assigned to Cu^{2+}–CO, whereas bands in the range $2160-2080\ cm^{-1}$ are attributed to Cu^{+}–CO. Cu^0 carbonyls including single-site and nanostructures species occur <2130 cm^{-1}.

CO adsorption on single crystal copper surfaces results in peaks ≤2100 cm^{-1} [34–37]. A difference of 26 cm^{-1} (2076–2102 cm^{-1}) in the stretching frequency of linearly adsorbed CO has been reported for different crystal facets [36]. Low frequency bands can be assigned to terrace places on low-indexed Cu surface planes. High frequency bands are due to CO adsorbed on high-indexed Cu surface planes or defect sites. CO stretching frequencies at $\nu(CO) = 1830$ and 1812 cm^{-1} have been associated with bridging species on the Cu(111) surface [37]. Furthermore, the band position of linearly adsorbed CO is affected by dipole coupling (blue shift with increasing coverage in absence of any variation in the electron exchange between the CO molecule and the metal) superimposed by gradual changes in the balance of σ- and π-bonding components [38].

In spite of these complications, good accordance has been generally detected between the spectra of CO adsorbed on single crystal Cu surfaces on the one hand and nano-structured copper particles supported on oxides on the other hand, [10, 14–18, 36] resulting in the general agreement that peaks >2100 cm^{-1} are ascribed to CO adsorption on oxidized copper species Cu^{n+}, while peaks <2100 cm^{-1} are due to CO adsorption on metallic copper.

According to XRD, the calcined precursors contain a CuO phase (tenorite) as the only semi-crystalline phase [21]. Adsorption of CO on copper oxide at room temperature generally leads to the formation of Cu^{+}–CO carbonyls [3]. In agreement with the literature, adsorption of CO on the reference CuO (Fig. S6) resulted in the formation of a weak signal at 2135 cm^{-1} that suggests the presence of Cu^{+}. This band was also found in the spectra of the calcined precursors (Fig. 1). However, it contributes only as a weak shoulder to the intense signals with maxima at 2100 cm^{-1}. Due to the nano-structured character of the calcined precursors, the surfaces consist of structurally/energetically different sites reflected in the low energy and broadness of the main peaks for CO adsorption on CuO/MgO and CuO/ZnO:Al, respectively. The peaks may contain several contributions. The signal of both calcined precursors at about 2100 cm^{-1} is proposed to be a result of partial surface reduction during calcination. From NEXAFS measurements at ambient pressure of the calcined CuO/ZnO:Al precursor, we know that a small fraction of CuO is already reduced to Cu_2O (Fig. S7). The partially reduced surface is probed by the adsorption of CO. Since no difference between the ZnO-containing and the ZnO-free calcined precursors was detected, the nano-structure of CuO in these materials is apparently comparable.

In contrast, major differences were observed after reduction of the two catalysts (Fig. 2). Cu/MgO displays mainly a CO adsorption band at 2089 cm^{-1} with a shoulder at 2060 cm^{-1} well in agreement with the presence of metallic Cu. Furthermore, from single crystal studies performed on differently oriented facets, it was inferred that closed packed surfaces as Cu(111) give rise to lower wavenumber signals at 2076 cm^{-1}, and more open facets as (100) and (110) lead to signals at higher wavenumbers 2085 and 2093 cm^{-1}, respectively [36]. The stretching frequency of CO on nano-structured, highly defective Cu surfaces is shifted to still higher wavenumbers [10, 15, 36]. The peak at 2089 cm^{-1} is consequently attributed to nano-structured metallic copper. The weak shoulder at 2114 cm^{-1}, only observed at high coverage in the measurement at 77 K, may indicate that the Cu component within a nano-structured Cu/metal oxide system is not completely reducible due to the intimate interfacial contact to the oxide part. CO adsorption was not found to take place on MgO at 300 K. A weak signal for CO adsorption on MgO is visible at a band position of 2180 cm^{-1} if the CO adsorption was performed at low temperatures (Fig. 4, right) [39].

Compared to Cu/MgO, the intensity of the signals due to CO adsorbed on Cu/ZnO:Al catalyst is drastically diminished by about one order of magnitude after reduction (Fig. 5, middle). The band maximum is located at 2125 cm^{-1}, which is neither typical for metallic Cu^0–CO nor resembling the

adsorption of CO on the calcined precursor or CuO. The signal contains several contributions including a component at 2090 cm^{-1} attributed to nano-structured metallic copper. Substantial coverage of the metallic copper surface in the reduced Cu/ZnO:Al catalyst would be one plausible explanation for the high energy of the peak maximum and the low intensity of the signal. From previous XPS studies it is known, that under reducing conditions the surface of Cu/ZnO:Al is highly enriched in Zn [21, 28]. Recent HR-TEM investigations provided further evidence for the formation of a zinc oxide overlayer [29]. Furthermore, we do not see any hints for a Cu-Zn surface alloy formation under the applied conditions of reduction. The band position for CO adsorption on a CuZn alloy (or brass) sample is expected to arise at the same position (2071 cm^{-1}) as metallic copper [40]. Adsorption of CO on ZnO at 77 K (Fig. S6, right) results in the formation of Zn^{2+}–CO band at 2188 – 2180 cm^{-1} [3]. The peaks usually disappear upon evacuation. Referring to the HR-TEM study, [29] the main peak at 2125 cm^{-1} is, therefore, tentatively attributed to adsorption of CO on the surface of a partially reduced ZnO overlayer ($Zn^{\delta+}$–CO) or alternatively to not completely reduced $Cu^{\delta+}$–CO species. Explicit discrimination between carbonyls of $Cu^{\delta+}$ and $Zn^{\delta+}$ is impossible based on the present experiments. The shoulder at 2112 cm^{-1} may be attributed to Cu defects, which are coordinatively and electronically unsaturated.

The stability of the carbonyls formed on Cu/ZnO:Al as well as on Cu/MgO is low. Consequently, the CO desorption experiment (Fig. 3) provides no further hints in terms of an assignment. Interestingly, the additional band at 1996 cm^{-1}, only observed on the ZnO-containing catalyst (Fig. 3, left), is stable in vacuum. Formation of a $CuZn_x$ surface alloy is unlikely under the applied conditions, [41] since the peak is not observed when CO is adsorbed on Cu/ZnO:Al reduced at higher temperatures. The assignment of the band at 1996 cm^{-1} requires further investigations. We may speculate at this point that the feature originates from adsorption of CO on the Cu-ZnO_{1-x} interface in a bridged position or on metallic Cu sites that are electronically modified by the interaction with ZnO_{1-x}.

In summary, the shift of the peak maximum of CO adsorbed on the reduced Cu/ZnO:Al catalyst to higher energies in comparison with Cu/MgO (Fig. 5, middle) indicates clearly that adsorption sites on metallic copper are largely not accessible in presence of ZnO, which may be interpreted in terms of a coverage of the metallic copper surface with defective zinc oxide species as a result of the reductive treatment [29]. The low intensity of the signal of adsorbed CO may be interpreted in terms of a limited number of adsorption sites on the surface of the partially reduced ZnO overlayer or, more likely, in terms of a different absorption coefficient of CO adsorbed on $Zn^{\delta+}$–CO compared to Cu^0–CO [3]. Such a phenomenon is not observed when non-reducible MgO is used as matrix for nano-structured copper. At this point it should be emphasized again that the domain size of the metallic copper determined by XRD is comparable for the two reduced catalysts (Table 1).

Adsorption of CO on Cu/MgO at 77 K results in similar spectra as the adsorption of CO at room temperature, confirming an incompletely reduced character of Cu by the occurrence of a shoulder at 2114 cm^{-1} at high coverage. The partially oxidized Cu species are most probably located at the interface to the metal oxide (here MgO). This hypothesis is supported by the results of NEXAFS measurements (Fig. S8), showing a not complete metallic Cu L-edge even under 1 bar 10% hydrogen at 523 K.

In contrast, the spectra recorded at 300 and 77 K on the reduced Cu/ZnO:Al catalyst differ in terms of the peak positions, and also in intensity (Fig. 5, right). The main signal observed at 77 K at low CO coverage is located at 2096 cm^{-1} and can be attributed to metallic copper. Hence, contrary to the measurement at room temperature, where the Cu surface seemed to be almost completely blocked by the layered ZnO polymorph, Cu is exposed at least partly to gas phase CO at 77 K. One explanation is, that the ZnO overlayer cracked mechanically due to different thermal expansion coefficients of Cu metal and ZnO when the reduced catalyst is cooled down to 77 K. Only at higher CO pressures the overlayer becomes slowly visible again indicating that the encapsulation of Cu is re-established (Fig. 4, left). It has been reported that under reducing conditions, ZnO in contact with Cu becomes mobile leading to rearrangements [25].

5 Conclusions

In the present contribution the surface of copper embedded in a matrix of either ZnO:Al or MgO has been studied by DRIFT spectroscopy applying carbon monoxide as probe molecule. It was found, that the adsorption of CO on metallic copper is substantially suppressed after activation of the high-performance Cu/ZnO:Al catalyst by a reductive treatment at 523 K. In contrast, nano-structured metallic copper is accessible for gas-phase CO in the reduced Cu/MgO catalyst. The signal of adsorbed CO that was detected for the ZnO-containing catalyst differs from the signal usually observed after adsorption of CO on metallic copper. The results are in agreement with the adsorption of CO on $M^{\delta+}$ (M = Zn, Cu, but most likely Zn) due to the formation of a thin layer of metastable “graphitic -/ boron nitride-like” ZnO on top of the metallic Cu particles previously detected by HR-TEM [29]. The DRIFTS study indicates that the local observation made by HR-TEM is representative for the entire catalyst surface. The coverage of metallic copper is not complete. Furthermore, our study shows that within a nanostructured Cu/metal oxide system, the Cu-moieties are

not completely reducible, most probably at the interfacial contact of the metal and the metal oxide. The importance of the Cu/ZnO interface in reverse water–gas shift and methanol synthesis reactions was recently evidenced [42, 43].

The differences observed in methanol synthesis reactivity between ZnO-containing and ZnO-free catalysts in their active states could be related to a different nature of the surfaces that are exposed to the gas phase. The results demonstrate a step further towards an improved understanding of the synergistic effects in Cu-ZnO based catalyst for methanol synthesis. In the present study reduced catalysts have been studied. The surface may change under reaction conditions [42]. Therefore, DRIFTS investigations of used catalysts transferred to the measurement cell without air contact and DRIFTS studies under operation at 30 bar pressure are currently underway.

Acknowledgements Open access funding provided by Max Planck Society.

References

1. Zaera F (2014) New advances in the use of infrared absorption spectroscopy for the characterization of heterogeneous catalytic reactions. Chem Soc Rev 43:7624–7663
2. Lamberti C, Zecchina A, Groppo E, Bordiga S (2010) Probing the surfaces of heterogeneous catalysts by in situ IR spectroscopy. Chem Soc Rev 39:4951–5001
3. Hadjiivanov KI, Vayssilov GN (2002) Characterization of oxide surfaces and zeolites by carbon monoxide as an IR probe molecule. Adv Catal 47:307–511
4. Knözinger H (2008) Infrared spectroscopy for the characterization of surface acidity and basicity. Handbook of heterogeneous catalysis. Wiley, New Jersey
5. Hadjiivanov K, Knözinger H (2009) Characterization of vacant coordination sites of cations on the surfaces of oxides and zeolites using infrared spectroscopy of adsorbed probe molecules. Surf Sci 603:1629–1636
6. Zaera F (2012) Infrared absorption spectroscopy of adsorbed co: new applications in nanocatalysis for an old approach. ChemCatChem 4:1525–1533
7. Bordiga S, Lamberti C, Bonino F, Travert A, Thibault-Starzyk F (2015) Probing zeolites by vibrational spectroscopies. Chem Soc Rev 44:7262–7341
8. Carenco S (2014) Carbon monoxide-induced dynamic metal-surface nanostructuring. Chem Eur J 20:10616–10625
9. Sun Q, Liu C-W, Pan W, Zhu Q-M, Deng J-F (1998) In situ IR studies on the mechanism of methanol synthesis over an ultrafine Cu/ZnO/Al2O3 catalyst. Appl Catal A 171:301–308
10. Sakakini BH, Tabatabaei J, Watson MJ, Waugh KC (2000) Structural changes of the Cu surface of a Cu/ZnO/Al_2O_3 catalyst, resulting from oxidation and reduction, probed by CO infrared spectroscopy. J Mol Catal A 162:297–306
11. Martin O, Mondelli C, Cervellino A, Ferri D, Curulla-Ferré D, Pérez-Ramírez J (2016) Operando synchrotron X-ray powder diffraction and modulated–excitation infrared spectroscopy elucidate the CO_2 promotion on a commercial methanol synthesis catalyst. Angew Chem Int Ed 55:11031–11036
12. Bailey S, Froment GF, Snoeck JW, Waugh KC (1994) A DRIFTS study of the morphology and surface adsorbate composition of an operating methanol synthesis catalyst. Catal Lett 30:99–111
13. Kanai Y, Watanabe T, Fujitani T, Saito M, Nakamura J, Uchijima T (1994) Evidence for the migration of ZnOx in a Cu/ZnO methanol synthesis catalyst. Catal Lett 27:67–78
14. Bailie JE, Rochester CH, Millar GJ (1995) Spectroscopic evidence for adsorption sites located at Cu/ZnO interfaces. Catal Lett 31:333–340
15. Topsøe N-Y, Topsøe H (1999) FTIR studies of dynamic surface structural changes in Cu-based methanol synthesis catalysts1. J Mol Catal A 141:95–105
16. Naumann d'Alnoncourt R, Bergmann M, Strunk J, Löffler E, Hinrichsen O, Muhler M (2005) The coverage-dependent adsorption of carbon monoxide on hydrogen-reduced copper catalysts: the combined application of microcalorimetry, temperature-programmed desorption and FTIR spectroscopy. Thermochim Acta 434:132–139
17. Naumann d'Alnoncourt R, Xia X, Strunk J, Loffler E, Hinrichsen O, Muhler M (2006) The influence of strongly reducing conditions on strong metal-support interactions in Cu/ZnO catalysts used for methanol synthesis. Phys Chem Chem Phys 8:1525–1538
18. Millar GJ, Rochester CH, Waugh KC (1991) Infrared study of CO adsorption on reduced and oxidised silica-supported copper catalysts. J Chem Soc Faraday Trans 87:1467–1472
19. Yang Y, Mei D, Peden CHF, Campbell CT, Mims CA (2015) Surface-Bound intermediates in low-temperature methanol synthesis on copper: participants and spectators. ACS Catal 5:7328–7337
20. Zander S, Kunkes EL, Schuster ME, Schumann J, Weinberg G, Teschner D et al (2013) The role of the oxide component in the development of copper composite catalysts for methanol synthesis. Angew Chem Int Ed 52:6536–6540
21. Schumann J, Lunkenbein T, Tarasov A, Thomas N, Schlögl R, Behrens M (2014) Synthesis and characterisation of a highly active Cu/ZnO:Al catalyst. ChemCatChem 6:2889–2897
22. Studt F, Behrens M, Kunkes EL, Thomas N, Zander S, Tarasov A et al (2015) The mechanism of CO and CO_2 hydrogenation to methanol over Cu-based catalysts. ChemCatChem 7:1105–1111
23. Kanai Y, Watanabe T, Fujitani T, Uchijima T, Nakamura J (1996) The synergy between Cu and ZnO in methanol synthesis catalysts. Catal Lett 38:157–163
24. Spencer MS (1999) The role of zinc oxide in Cu/ZnO catalysts for methanol synthesis and the water–gas shift reaction. Top Catal 8:259–266
25. Grunwaldt JD, Molenbroek AM, Topsøe NY, Topsøe H, Clausen BS (2000) In situ investigations of structural changes in Cu/ZnO catalysts. J Catal 194:452–460
26. Jansen WPA, Beckers J, Heuvel JC, Denier VD, Gon AW, Bliek A, Brongersma HH (2002) Dynamic behavior of the surface structure of Cu/ZnO/SiO_2 catalysts. J Catal 210:229–236
27. Liao F, Huang Y, Ge J, Zheng W, Tedsree K, Collier P et al (2011) Morphology–dependent interactions of ZnO with Cu nanoparticles at the materials' interface in selective hydrogenation of CO_2 to CH_3OH. Angew Chem Int Ed 50:2162–2165
28. Behrens M, Studt F, Kasatkin I, Kühl S, Hävecker M, Abild-Pedersen F et al (2012) The active site of methanol synthesis over Cu/ZnO/Al2O3 industrial catalysts. Science 336:893–897
29. Lunkenbein T, Schumann J, Behrens M, Schlögl R, Willinger MG (2015) Formation of a ZnO overlayer in industrial Cu/ZnO/Al2O3

catalysts induced by strong metal–support Interactions. Angew Chem Int Ed 54:4544–4548
30. Sirita J, Phanichphant S, Meunier FC (2007) Quantitative analysis of adsorbate concentrations by diffuse reflectance FT-IR. Anal Chem 79:3912–3918
31. Olinger JM, Griffiths PR (1988) Quantitative effects of an absorbing matrix on near-infrared diffuse reflectance spectra. Anal Chem 60:2427–2435
32. Kortüm G, Braun W, Herzog G (1963) Principles and techniques of diffuse-reflectance spectroscopy. Angew Chem Int Ed 2:333–341
33. Fichtl MB, Schumann J, Kasatkin I, Jacobsen N, Behrens M, Schlögl R et al (2014) Counting of oxygen defects versus metal surface sites in methanol synthesis catalysts by different probe molecules. Angew Chem Int Ed 53:7043–7047
34. Eischens RP, Pliskin WA (1958) The infrared spectra of adsorbed molecules. In: Advances in catalysis Eley WGFVIK DD, Paul BW pp 1–56. Academic Press, Cambridge
35. Smith AW, Quets JM (1965) Adsorption of carbon monoxide on copper. J Catal 4:163–171
36. Pritchard J, Catterick T, Gupta RK (1975) Infrared spectroscopy of chemisorbed carbon monoxide on copper. Surf Sci 53:1–20
37. Hayden BE, Kretzschmar K, Bradshaw AM (1985) An infrared spectroscopic study of CO on Cu(111): the linear, bridging and physisorbed species. Surf Sci 155:553–566
38. Hollins P, Pritchard J (1979) Interactions of CO molecules adsorbed on Cu(111). Surf Sci 89:486–495
39. Spoto G, Gribov EN, Ricchiardi G, Damin A, Scarano D, Bordiga S et al (2004) Carbon monoxide MgO from dispersed solids to single crystals: a review and new advances. Prog Surf Sci 76:71–146
40. Schott V, Oberhofer H, Birkner A, Xu M, Wang Y, Muhler M et al (2013) Chemical activity of thin oxide layers: strong interactions with the support yield a new thin-film phase of ZnO. Angew Chem Int Ed 52:11925–11929
41. Liu Z, Rittermeier A, Becker M, Kähler K, Löffler E, Muhler M (2011) High-pressure CO adsorption on Cu-based catalysts: Zn-induced formation of strongly bound CO monitored by ATR-IR spectroscopy. Langmuir 27:4728–4733
42. Lunkenbein T, Girgsdies F, Kandemir T, Thomas N, Behrens M, Schlögl R et al (2016) Bridging the time gap: a copper/zinc oxide/aluminum oxide catalyst for methanol synthesis studied under industrially relevant conditions and time scales. Angew Chem Int Ed. doi:10.1002/anie.201603368
43. Álvarez Galván C, Schumann J, Behrens M, Fierro JLG, Schlögl R, Frei E (2016) Reverse water–gas shift reaction at the Cu/ZnO interface: influence of the Cu/Zn ratio on structure-activity correlations. Appl Catal B 195:104–111